Low Temperature Physics/Fizika Nizkikh Temperatur, 2018, v. 44, No. 2, pp. 154–167

Thermodynamics of dilute ^{3}He–^{4}He solid solutions with hcp structure

K.A. Chishko

B. Verkin Institute for Low Temperature Physics and Engineering of the National Academy of Sciences of Ukraine
47 Nauky Ave., Kharkiv 61103, Ukraine
E-mail: chishko@ilt.kharkov.ua

Received June 4, 2017, revised August 8, 2017, published online December 25, 2017

To interpret the anomalies in heat capacity $C_V(T)$ and temperature-dependent pressure $P(T)$ of solid hexagonal close-packed (hcp) ^{4}He we exploit the model of hcp crystalline polytype with specific lattice degrees of freedom and describe the thermodynamics of impurity-free ^{4}He solid as superposition of phononic and polytypic contributions. The hcp-based polytype is a stack of 2D basal atomic monolayers on triangular lattice packed with arbitrary long (up to infinity) spatial period along the hexagonal c axis perpendicular to the basal planes. It is a crystal with perfect ordering along the layers, but without microscopic translational symmetry in perpendicular direction (which remains, nevertheless, the rotational crystallographic axis of third order, so that the polytype can be considered as semi-disordered system). Each atom of the hcp polytype has twelve crystallographic neighbors in both first and second coordination spheres at any arbitrary packing order. It is shown that the crystal of such structure behaves as anisotropic elastic medium with specific dispersion law of phonon excitations along c axis. The free energy and the heat capacity consist of two terms: one of them is a normal contribution (with $C_V(T) \sim T^3$) from phonon excitations in an anisotropic lattice of hexagonal symmetry, and another term (an "excessive" heat) is a contribution resulted by packing entropy from quasi-one-dimensional system of 2D basal planes on triangular lattice stacked randomly along c axis without braking the closest pack between neighboring atomic layers. The excessive part of the free energy has been treated within 1D quasi-Ising (lattice gas) model using the transfer matrix approach. This model makes us possible to interpret successfully the thermodynamic anomaly (heat capacity peak in hcp ^{4}He) observed experimentally.

PACS: 67.80.B– Solid ^{4}He;
05.70.–a Thermodynamics;
61.72.Nn Stacking faults and other planar or extended defects.

Keywords: polytype, packing entropy, quantum solids.

1. Introduction

Thermodynamical and mechanical properties of hexagonal close-packed (hcp) ^{4}He crystals are the subject matter of lively discussions over last decade in the context of the unusual peculiarities in behavior of these quantum solids at low temperature. There are well-known anomalies in temperature dependences of pressure $P(T)$ [1,2] and heat capacity $C_V(T)$ [3–6] (it is noticeable that anomalous behavior of hcp ^{4}He heat capacity below 0.5 K was reported also in the paper of Edwards and Pandorf [7]) as well as in mechanical (mainly acoustical [8–10]) properties investigated with different (especially with torsion oscillator [11,12] or internal friction [13,14]) technics. It is remarkable that both the thermodynamical [1,3] and mechanical (acoustical) anomalies appear just below 0.25 K, and this fact most likely suggests that they are phenomena of the common nature. For this moment it is agreed that all the relevant observations are results of some structural disorder created by crystal lattice defects (dislocations [6,11,15–19] or vacancies [20–24]).

Whereas a dislocation concept seems to be quite satisfactory to explain mechanical behavior (plasticity) of the helium lattice in torsion oscillator, it is unsuccessful in treatment of thermodynamic anomalies like low-temperature heat capacity peak [3] or low-temperature non-monotonic increase in pressure with temperature [1] obtained in pure ^{4}He crystals, but not observable in ^{3}He. The specific effect of ^{3}He impurities in ^{4}He matrix (hysteresis in $C_V(T)$ during thermocycling) becomes detectable over the heat capacity peak only at impurity concentration greater than several ppm [3]. Moreover, it remains unclear what is the reason for absence of essential dislocation effects in low-pressure body-centered cubic (bcc) ^{3}He solid treated with torsion oscillator [2] (according to accepted meanings, the cubic

lattice must have more easy glide systems as compared to hcp lattice [25,26]). Dislocation is one-dimensional non-equilibrium defect with specific oscillatory degrees of freedom, so that to get an essential contribution from dislocations to the heat capacity in three-dimensional lattice we have to suggest the presence of an enormous dislocation density (of order 10^{11}cm^{-2}) which is hardly to be conceived in the quantum helium crystal. It means that to explain the low-temperature anomalies in thermodynamics of the pure ^{4}He lattice we have to propose a model which based essentially on its hcp crystallography. The contribution from dislocations into observable properties of solid helium is a subject of extensive studies over last years [27–30], but it is very difficult to obtain some direct evidence of the dislocations response in such systems because of specifics of helium crystals prepared in restricted volume under external pressure at ultralow temperature.

Another approach to explain the anomalies in thermodynamics of ^{4}He solid is a glassy phase model [31,32]. To interpret the supersolidity effects, this model was introduced by Andreev [33] on basis of simple two-level system traditionally applicable to description of disorder in various glassy objects. The mentioned approach makes it possible to involve additional (to the natural phonon ones) degrees of freedom and create the qualitative explanation [31,32] for local maximum on heat capacity curve $C_V(T)$ [3]. Nevertheless, it remains unclear the nature of the glassy degrees in view of their relation to the real degrees of freedom of ^{4}He atoms in the helium crystal lattice.

As alternative to ordinary dislocation concept and glassy approach we propose [34,35] the model of hcp polytype [36–38] which made us possible to explain successfully the anomalies in temperature dependences of pressure reported in Refs. 1, 2. The advantage of the polytypic model is the strongly determined crystallographic structure of hcp polytype with evident physical nature of the packing degrees in a stack of basal planes which are crystallographically perfect monoatomic layers with triangular lattice. This model makes it possible to realize a mechanism of one-dimensional order-disorder transformation in a perfectly close-packed three-dimensional hcp crystal. Here we apply the corresponding theory to clarify the experimentally observed in [3] low-temperature heat capacity peak that exists due to specific degrees of freedom of the hcp lattice. This effect seems to be evidently independent on both phononic and impuritonic degrees, so that we suggest another mechanism for explanation of the phenomenon.

Heat capacity anomaly in solid ^{4}He discovered experimentally by Chan's research group [3] is an excessive specific heat (in addition to standard T^3 law) at temperature below 0.2 K. The local heat capacity peak is observable clearly even in ^{4}He of the highest purity where the possibly effect of ^{3}He isotope seems to be evidently negligible. The magnitude of the anomalous peak is higher in the sample grown during 4-hrs procedure (as compered to 20-hrs one), or in the sample grown at lower external pressure of 33 bar (as compared to 38 bar one). If we believe that the appearance of the peak is connected with some crystal lattice defects then it is quite reasonable to suggest that the crystalline sample is more perfect being grown with smaller growth rate or at higher external pressure. However, the nature of these defects is up to now a matter of worldwide discussions [31,32].

To interpret this phenomenon we propose to include into description, beyond standard phonon oscillations, a contribution from some additional degrees of freedom (cmp with Ref. 31), and these degrees are undoubtedly elements of lattice structural transformations at low temperatures. The polytypic model makes us possible to elaborate the real physical mechanism for clarification of the unexpected thermodynamical and mechanical behavior demonstrated by the hcp solid ^{4}He at the low-temperature region. It is shown in [34] that hcp polytype can be interpreted as anisotropic elastic continuum with specific dispersion law in c direction due to one-dimensional disorder in packing of the polytype stack. After simple averaging procedure [34] (it corresponds to the long-wave approximation, which is quite natural as to the solid helium where the Debye temperature is of order higher as the melting temperature of the crystal) the system is reduced to anisotropic elastic continuum with crystallographic symmetry of hexagonal subgroup C^1_{3v} (it should be emphasized that it is transversally-isotropic elastic medium). The excitation of the continuum are standard phonons, but situation becomes more sophisticated if the intrinsic structure of the multilayered polytype is taken into account. The 1D packing order in the polytype stack changes with temperature, so that the corresponding (non-phononic) degrees of freedom contribute to the total free energy of the system. At low temperature both phononic $(F_{\rm ph}(T))$ and polytypic $(F_{\rm poly}(T))$ parts of the free energy $(F_{\rm tot}(T) = F_{\rm ph}(T) + F_{\rm poly}(T))$ are comparable small but $F_{\rm poly}(T)$ decreases with temperature quite rapidly, and above approximately 0.2 K we can see the only ordinary phonon contribution $F_{\rm tot} \sim T^4$ (and, correspondingly, the heat capacity $C_V \sim T^3$ and pressure $P(T) \sim T^4$). As a result, the dependence $C_V(T)$ has the local maximum, and, respectively, $P(T)$ is locally non-monotonic (inflection point on the curve $P(T)$ [35]) in the vicinity of 0.1–0.2 K.

The paper is built as follows. Section 2 gives the statement of the problem. In Sec. 3, the phononic (Sec. 3.1) and polytypic (Sec. 3.2) parts of the total heat capacity $C_V(T)$ in polytypic crystal have been calculated. In Sec. 4 we compare and interpret the experimental data [3] in view of conclusions given by our theory. Section 5 contains the general discussion, and Section 6 is a brief conclusion.

2. Statement of the problem

A perfect monoatomic hcp crystal can be built as multilayered system [36–38] which is a stack of close-packed basal planes on triangular lattice (Fig. 1). According to the standard crystallographic procedure, we denote one of the

planes as A, and place a second element over the first one in such a way as not to destroy the closest packing of neighboring atoms in the whole stack.

This can be done in one of two positions as it is illustrated by Fig. 1(a) (B position over A layer) and Fig. 1(b) (C position over A layer). Thus, placing N two-dimensional basal elements in the mentioned manner, we can produce 2^N different polytype modifications of monoatomic crystal lattice where each atom has twelve nearest neighbors in the first coordination sphere and twelve next-nearest neighbors in the second coordination sphere, respectively, at any arbitrary sequence of A,B,C elements (and neighborhood of two coinciding elements is forbidden). The closest-packing principle is provided for any type of the polytypic structure [37], and the limit of entropy for the totally random packing of the polytype built of N 2D layers on triangular lattice is equal to $N\ln 2$. The two-plane periodic structure $...B\,|\,AB\,|\,A...$ is hexagonal close-packed (hcp or 2H) lattice, the three-plane period $...C\,|\,ABC\,|\,A...$ means face-centered cubic crystal (fcc or 3C). The next periodic polytypes are twinned hexagonal structures $...C\,|\,ABAC\,|\,A...$ (4H), and $...B\,|\,ABCAB\,|\,A...$ (5H) as well as six-layered modifications $...B\,|\,ABCACB\,|\,A...$ ($6H_1$) and $...C\,|\,ABABAC\,|\,A...$ ($6H_2$). Then are seven nine-periodic structures ($9T_{1...6}$ and 9R), twelve-periodic (12R), etc., up to a sequence of unlike-pairs with period formally tending to infinity [36–38] (the so-called random stacking faults or chaotic stacking faults structure). Any polytypic system can be obtained from the simplest 2H structure due to coherent elementary glide along the basal directions. In fact, it is the well-known mechanism of martensitic transformations in crystalline solids [37,38], and this fact can be illustrated by Fig. 2.

Figure 2 shows the layer A with "islands" of B and C types (for simplicity, we suppose the third overlayer is of A type similar to the first one). It can be seen that each island is surrounded by a channels due to incompatibility between B and C positions on the same A-substrate. These channels are network of Shockley's partial dislocations. If one boundary atom from island B jumps between two equivalent potential wells along the groove of the potential relief of the substrate (layer A) onto boundary of layer C, it means an elementary local displacement of the dislocation line through the distance $a/\sqrt{3}$ (where a is interatomic distance). After this act the island C increases, but island B decreases by one atom. Due to low energy of the barrier between neighboring B and C positions the mentioned displacement can be realized by quantum tunneling without thermal activation. This mechanism produces additional (as compared with phonon ones) degrees of freedom. The quantum tunneling along the real channel of the partial dislocation is possible due to Andreev–Lifshits mechanism, so that it gives us an explanation of restricted one-dimensional diffusion evidently observed in helium crystals [39–41].

In this connection the polytype of arbitrary structure is the hcp lattice with a certain one-dimensional distribution of "stacking faults" along c axis of hexagonal cell (perpendicular to basal planes). The faults are not, in fact, the defects, but only a certain arrangement and re-arrangement in succession of two-type crystalline planes with triangular lattice packed in a stack without breaking of 3D closest packing as a whole. The re-arrangement of such a stacks needs to get a certain stacking-fault energy (SFE) [42] and packing entropy, so that it is thermodynamically specified process with an average packing period in z direction as

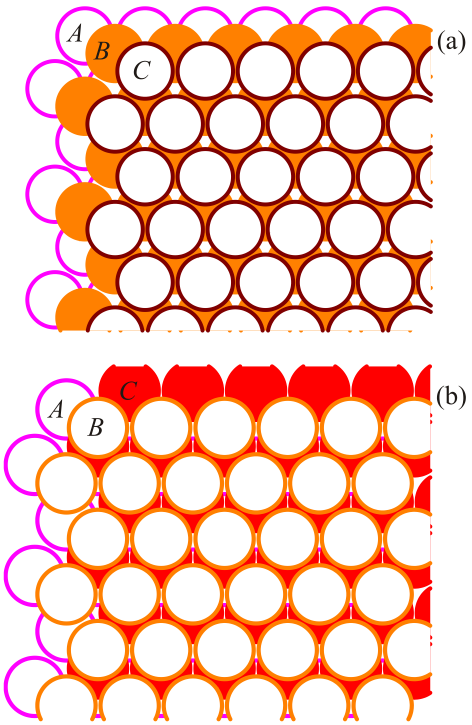

Fig. 1. (Color online) Three monoatomic layers on triangular lattice in two different position: …*ABC*… stack (a) and …*ACB*… stack (b).

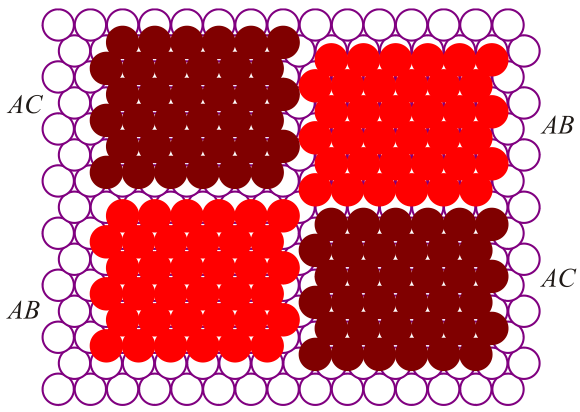

Fig. 2. (Color online) Different positions of *B*-type and *C*-type clusters on an *A*-type layer (schematic). The clusters divided by Shockley's partial dislocations (see text).

the order parameter of the spatially disordered crystal. The SFE is typically small in atomic and molecular cryocrystals, especially for solid helium, so that we can expect that the polytype model is perfectly suitable for solid ^{4}He.

To classify the polytypic structure we use below the more compact notation system of Ewald–Belov–Jagodzinski [37,38] which takes into account directly the local symmetry of crystalline environment for each site of a chosen 2D layer. So, if any layer A is surrounded by like-pair of neighbors (as BAB or CAC, etc.) then it means the position with local hexagonal symmetry, and this position we denote as *h* layer. If the layer is surrounded by unlike-pair (as BAC or CAB, etc.), we denote it as cubic or *c* layer. With this notation, for example, the $6H_1$ polytype should be denoted as $...|hcchcc|...$, etc. This notation system is more suitable for our goals in the present paper.

The stack of basal planes with totally aperiodic (random) packing without breaking the closest-packing principle is the system of random (or chaotic) stacking-faults (RSF) [38]. Evidently, this system does not possess a microscopic translation symmetry along *c* axis, but even in this case the direction perpendicular to basal planes remains the crystallographic axis of the third-order rotation symmetry. Thus, all the long-periodic polytypic structures (up to RSF) belong to hexagonal symmetry subgroup C_{3v}. As a result, in long-wave limit (it is just the case of solid ^{4}He) the polytype is crystallographycally perfect anisotropic elastic medium with hexagonal symmetry and specific dispersion of acoustic (phononic) excitation along *c* direction. Each variant of the polytypic stack has a specific intrinsic energy (due to SFE of individual elements in stack) and specific entropy (due to variety of packing configurations among N planes). In general, it is a complicated problem to be solved exactly, but in reality the anomalous heat capacity peak is comparably small, so that it is reasonable to suggest [31] that the total specific heat of the system is a result of additive contributions from phonons and some extraneous (non-phononic) degrees of freedom. The only question is the nature of these extraneous degrees which are supposed in [31] to be built of hypothetic two-level Andreev systems [33].

We will keep, in fact, the similar point of view but with the only difference that we propose the real physical mechanism of extraneous degrees based on a structural transformation in hcp crystalline polytype [37,38]. In this connection we need also re-calculate the spectrum of phonon excitations in a polytypic crystal. By this means the free energy $F(T,V)$ of the polytype consists of two parts,

$$F(T,V) = F_{\text{ex}}(T,N) + F_{\text{ph}}(T,V), \qquad (1)$$

where $F_{\text{ph}}(T,V)$ is the "dynamic" part due to phonon excitation in anisotropic lattice, and $F_{\text{ex}}(T,N)$ is the excessive or "static" part as the free energy of a multilayered stack built of two-dimensional closely-packed atomic layers on triangular lattice. Successive transformation with temperature and pressure in solid polytype is realized as a continuous solid phase transition of martensitic type through a chain of phases with different spatial periods along *c* axis. The phases can be short-periodic, long-periodic [43–46] and even aperiodic (RSF). It means, that phonon spectrum of the crystal depends on the details of its polytypic structure and, as a result, the free energy Eq. (3) could not be, in general, presented as superposition of phonon and polytypic part. However, taking into account that any polytypic transformation in the stack of the layers with triangular lattice do not destroy the close packing of the crystal which remains macroscopically perfect elastic medium, and only long-wave phonons are essential for thermodynamics of helium solids, we conclude that the model of Eq. (1) is valid to describe the system under study.

3. Heat capacity of hcp ^{4}He polytype

Crystallographic structure and physical properties of polytypes have been detailed in Refs. 37, 38. The phonon spectrum and thermodynamics of the ^{4}He polytype have been studied in Ref. 34. The isochoric heat capacity of the crystal is

$$C_V(T) = T\left(\frac{\partial S}{\partial T}\right)_V = -T\left(\frac{\partial^2 F(T,V)}{\partial T^2}\right)_V =$$

$$= C_{\text{ex}}(T) + C_{\text{ph}}(T), \qquad (2)$$

where $S = -(\partial F(T,V)/\partial T)_V$ is the entropy. Below we calculate C_{ph} and C_{ex}.

3.1. Phonon part of heat capacity

The general expression for the function $F_{\text{ph}}(T)$ is well known [47–49]:

$$F_{\text{ph}}(T) = \sum_{\mathbf{k},\alpha}\left\{\frac{\omega_\alpha(\mathbf{k})}{2} + T\ln\left[1-\exp\left(-\beta\omega_\alpha(\mathbf{k})\right)\right]\right\}, \qquad (3)$$

where the summation is over all states in the Brillouin zone, and all three acoustic frequency branches $\omega_\alpha(\mathbf{k})$ $(\alpha = 1, 2, 3))$ of the spectrum in monoatomic lattice (we use the system of units with Planck and Boltzmann constants equal to one, $\mathbf{k}$ is three-dimensional wave vector), and $\beta = 1/T$. To get the spectrum $\omega_\alpha(\mathbf{k})$ we solve the corresponding problem of lattice dynamics [49] within harmonic approximation with only interaction of the nearest neighbors. It is shown in [34] that hcp polytype can be interpreted as anisotropic elastic continuum with specific dispersion law in direction of disordered *c* axis. The averaging procedure consists in replacement of the finite differences describing interatomic interactions along *c* axis by spatial derivatives of corresponding order. As a result, it means the passage to long-wave approximation, and such a procedure is quite natural as to the solid helium where the

Debye temperature is of order higher as the melting temperature of the crystal. Finally, the phononic free energy of the ^{4}He polytype can be written in the form [34,35] (V is the volume of the system, a is the interatomic distance and c is the period of ideal hcp lattice, $\gamma = c/a$)

$$F_{\rm ph}(T) = \frac{2TV}{\pi\gamma a^3} \sum_{\nu=1,2,3} \int_0^{q_D} q dq \int_0^{\pi/2} dq_z \ln\left\{1 - \exp\left[-\beta\omega_\nu(q,q_z)\right]\right\}, \qquad V = \frac{\sqrt{3}}{4} N_{1D} N_{2D} \gamma a^3, \tag{4}$$

where N_{2D} is the number of atoms in an individual basal plane on triangular lattice, N_{1D} is the total number of the basal planes in the stack (so that $N_{1D}N_{2D}$ is the total number of atoms in the crystal), $q^2 = a^2(k_x^2 + k_y^2)$ is the two-dimensional wave vector in a basal plane, $q_z = ak_z$, and

$$k_D = \frac{1}{a}\sqrt{\frac{8\pi}{\sqrt{3}}}, \quad q_D = ak_D,$$

is the approximate Debye vector for the first Brillouin zone of triangular lattice [34,50] (it appears when the exact hexagonal zone of 2D lattice [51] is replaced by an equivalent circular area in **k** space).

After all these simplifications the spectrum of the problem [34,35] at the ideal ratio $\gamma = \sqrt{8/3} = 1.63$ can be written as

$$\omega_{1,2,3}(q,q_z) = \Omega\sqrt{Z_0\left(\varepsilon^2_{\omega_{1,2,3}}(q,q_z) + \frac{D_a}{4\Omega}q^2\right)}. \tag{5}$$

Here $Z_0 = 6$ is coordination number in a basal plane,

$$\Omega^2 = \frac{U''(a)}{2m}, \qquad D_a = \frac{U'(a)}{2ma}, \tag{6}$$

where $U(r)$ is the energy of interatomic interaction on interatomic distance r, and m is the atomic mass. In fact, for high-symmetric close-packed helium lattice with twelve neighbors in the first and second coordination spheres the non-central part of interatomic interaction is small, and $D_a/\Omega \ll 1$. In addition, in the long-wave limit (typical for solid helium) the most essential part of the phonon spectrum corresponds to the condition $q, qz \ll 1$. As a result, with quite enough accuracy we can neglect the second term under the square root sign in Eq. (5), so that

$$\omega_{1,2,3}(q,q_z) = \sqrt{Z_0}\,\Omega\varepsilon_{\omega_{1,2,3}}(q,q_z). \tag{7}$$

Furthermore,

$$\varepsilon^2_{\omega_1}(q,q_z) = \rho(q,q_z)\cos\frac{\tau(q,q_z)}{3};$$

$$\varepsilon^2_{\omega_{2,3}}(q,q_z) = \rho(q,q_z)\left(-\cos\frac{\tau(q,q_z)}{3} \pm \sqrt{3}\sin\frac{\tau(q,q_z)}{3}\right),$$

where

$$\rho(q,q_z) = \sqrt[6]{Q^2 + |Q^2 + P^3|},$$

$$\tau(q,q_z) = \arctan\frac{\sqrt{|Q^2 + P^3|}}{Q},$$

with

$$Q(q,q_z) = -\frac{c_2^3}{27} - \frac{c_2 c_1}{6} - \frac{c_0}{2}, \quad P(q,q_z) = -\frac{3c_1 + c_2^2}{9}. \tag{8}$$

The coefficients $c_i(q,q_z)$ can be obtained from the corresponding relations of Refs. 34, 35 at $\gamma = \sqrt{8/3}$, and they have the form

$$c_2(q,q_z) = \frac{1}{12}(5q^2 + q_z^2);$$

$$c_1(q,q_z) = -\frac{1}{1296}\left(\frac{211}{4}q^4 + 134q^2q_z^2 + 81q_z^4\right);$$

$$c_0(q,q_z) = \frac{1}{2592}\left(\frac{281}{54}q^6 + \frac{94}{3}q^4q_z^2 + 17q^2q_z^4 + 6q_z^2\right).$$

It can be seen that in the case of $\gamma = \sqrt{8/3}$ the parameter Ω is the only "elastic constant" of the problem, and all three eigenfrequencies $\omega_\alpha(q,q_z)$ (Eq. (7)) are proportional to its value. Below, the frequency Ω will be the only real fitting parameter to describe the bulk heat capacity of the system under study.

Finally, the phonon heat capacity can be written in the form [47–49]

$$\frac{C_{\rm ph}(T)}{k_B} = \frac{\sqrt{3}}{4\pi^2} N_{1D}N_{2D} \sum_{\alpha=1,2,3} \int_0^{ak_D} q dq \int_0^{\pi} dq_z \left(\frac{\beta\omega_\alpha(q,q_z)}{2}\right)^2 \sinh^{-2}\left(\frac{\beta\omega_\alpha(q,q_z)}{2}\right). \tag{9}$$

Figure 3 shows the temperature behavior of the heat capacity Eq. (9) at different values Ω. The slope angle of the curve $C_{\rm ph}(T)$ at low temperature decreases with increase in Ω. It can be seen from Fig. 3(a) that the heat capacity Eq. (9) tends to equipartition law at $T \to \infty$ with accuracy of about 2% ($C_{\rm ph}(\infty) = 3.058 N_{1D} N_{2D} k_B$) which seems to be quite acceptable, taken into account the made above approximations and the fact that we need to describe only the low-temperature dependence of the solid ^{4}He heat capacity. The low-temperature heat capacity (Figs. 3(b), (c)) demonstrate the perfect T^3-dependence which is characteristic to an ideal Debye lattice.

3.2. Excessive heat capacity of the polytype

Here we consider a quasi-one-dimensional stack of N_{1D} two-dimensional crystalline layers packed in arbitrary order, for example, *...hchhhcchcchh...*, etc. It is reasonable to suggest that interaction in like-pairs *...hh...* and *...cc...* should be different from one another, and the both are different from interaction in unlike-pair *...hc...*. The

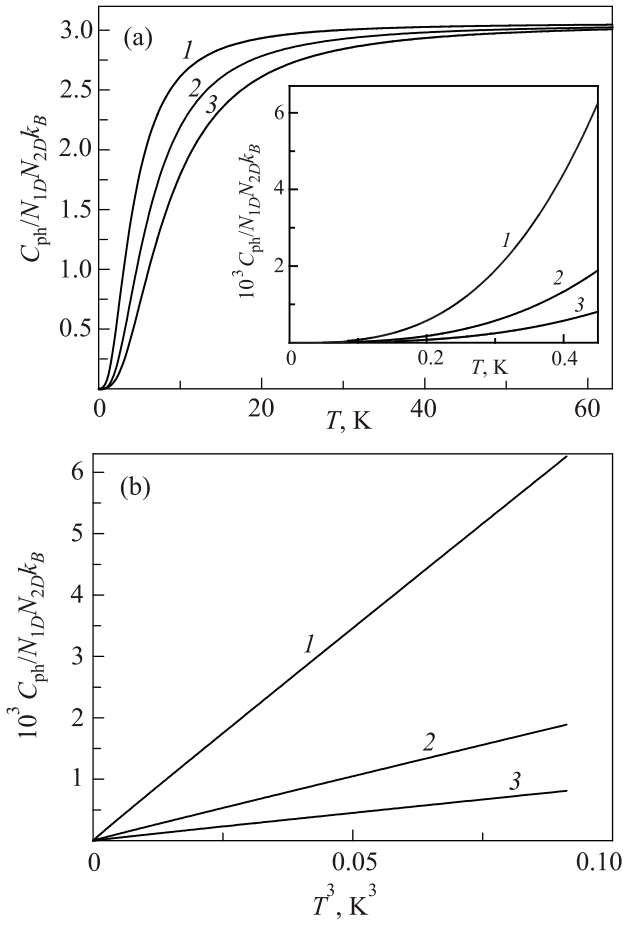

Fig. 3. The phonon part of the heat capacity of the polytype stack (per atom) for three values of Ω: 5 K (curve *1*), 7.5 K (curve *2*), 10 K (curve *3*). The inset on Fig. 3(a) presents the initial part of the corresponding dependences. Fig. 3(b) shows this part of the graph versus T^3-abscissa.

Hamiltonian of such system can be written as one-dimensional lattice gas model in the nearest neighbors approximation,

$$H_{\rm poly} = -\varepsilon_0 \sum_i \hat{\sigma}_i - V \sum_i \hat{\sigma}_i \hat{\sigma}_{i+1}, \tag{10}$$

where $\hat{\sigma}_i$ are "non-integer occupation numbers",

$$\hat{\sigma}_i = \begin{pmatrix} \sigma_c \\ \sigma_h \end{pmatrix} \tag{11}$$

which can take one of two values, $\sigma_c = 1 - \xi_c$ or $\sigma_h = 1 + \xi_h$ ($\xi_c, \xi_h \ll 1$), where ε_0 is the average energy per site, and $V > 0$ is an interaction energy between neighboring sites. This approach is a direct analog of exactly solving Ising model [52] as a chain of mutually coupled two-state systems. The difference between the proposed polytype model and an array of simple independent two-level systems (see Refs. 31, 33) is an account of interaction between neighboring basal planes.

The solution of the problem Eq. (10) can be obtained easily within transfer matrix approach [52,53]. The canonical partition function of the 1D problem is

$$Z_{1D} = {\rm Sp}\hat{\mathbf{T}}^{N_{1D}}, \quad \hat{\mathbf{T}} = \begin{pmatrix} \tau_{11} & \tau_{12} \\ \tau_{21} & \tau_{22} \end{pmatrix}, \tag{12}$$

where

$$\tau_{11} = \exp\left(a_0 \sigma_h + K\sigma_h^2\right), \quad \tau_{22} = \exp\left(a_0 \sigma_c + K\sigma_c^2\right),$$

$$\tau_{12} = \tau_{21} = \exp\left[\frac{a_0}{2}(\sigma_h + \sigma_c) + K\sigma_h\sigma_c\right], \tag{13}$$

and $a_0 = \beta\varepsilon_0$, $K = \beta V$. If $N_{1D} \gg 1$ then the excessive part of the free energy in Eq. (1) is equal to

$$F_{\rm ex}(T, N_{1D}) = -T \ln Z_{1D} = -N_{1D} T \ln \Lambda(T), \tag{14}$$

where $\Lambda = \max\{\lambda_1, \lambda_2\}$ is the greatest eigenvalue of the transfer matrix $\hat{\mathbf{T}}$. In the case of 2×2 matrix (Eq. (14)) we have [54]

$$\lambda_1 = \tau_{11} - \tau_{12} v, \quad \lambda_2 = \tau_{22} + \tau_{12} v, \tag{15}$$

where

$$v = p + {\rm sign}\, p \sqrt{1 + p^2}, \quad p = \frac{\tau_{22} - \tau_{11}}{2\tau_{12}}. \tag{16}$$

As a result, the static part of the heat capacity (per one basal plane) can be written in the form

$$\frac{C_{\rm ex}(T)}{k_B N_{1D}} = T \frac{\partial^2}{\partial T^2} \{T \ln \Lambda(T)\} =$$

$$= \frac{T}{\Lambda(T)} \left\{ \frac{\partial \Lambda(T)}{\partial T} \left[2 - \frac{T}{\Lambda(T)} \frac{\partial \Lambda(T)}{\partial T} \right] + T \frac{\partial^2 \Lambda(T)}{\partial T^2} \right\}. \tag{17}$$

Figure 4 shows the dependences $C_{\rm ex}(T)/k_B N_{1D}$ at different values of the parameters (all the values are clarified in the figure caption). The calculated excessive heat capacity $C_{\rm ex}(T)$ tends to zero at $T \to 0$ and $T \to \infty$, so that it undoubtedly has a maximum at intermediate temperatures. As a result, the total heat capacity Eq. (2) demonstrates the local maximum at low temperatures. With more detailes this fact is discussed in the next section.

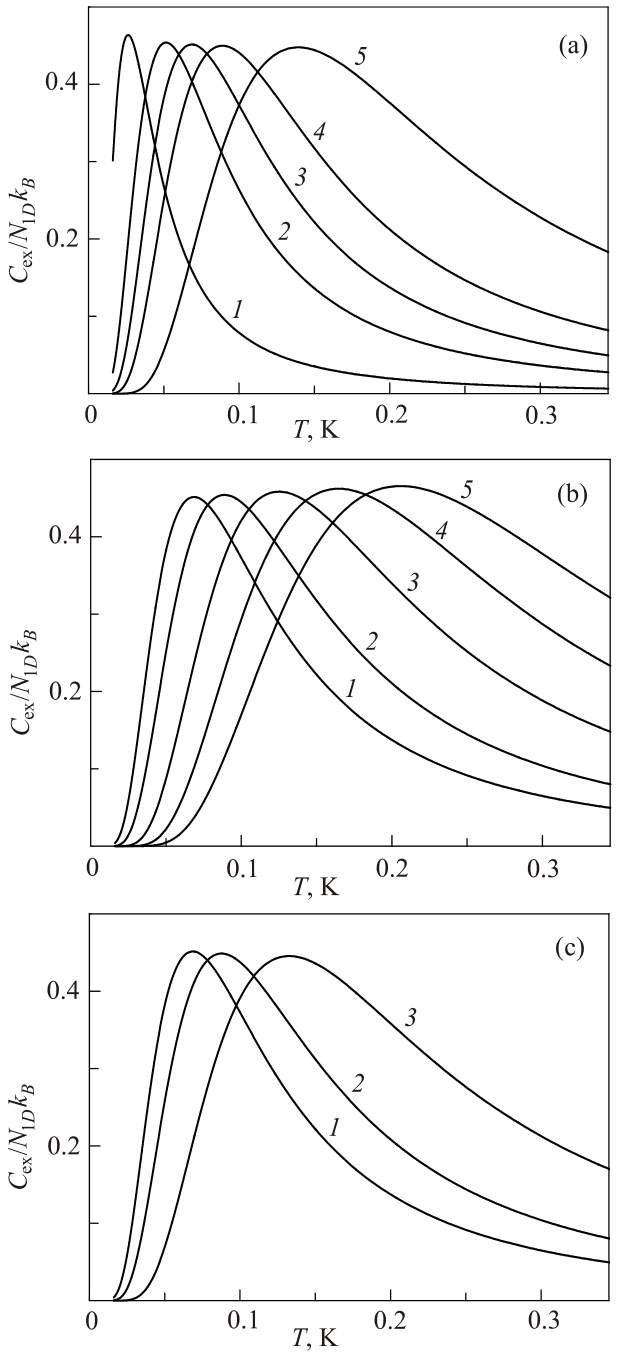

Fig. 4. Excessive heat capacity (per one basal plane): (a) $\xi_h = 0.05$, $\xi_c = 0.01$, $\varepsilon_0 = 4.01$ K, and $V = 2.51$ K (*1*), 3.01 K (*2*), 3.35 K (*3*), 3.75 K (*4*), 4.75 K (*5*); (b) $\xi_h = 0.05$, $\varepsilon_0 = 4.01$ K, $V = 3.35$ K and $\xi_c = 0.01$ (*1*), 0.025 (*2*), 0.05 (*3*), 0.075 (*4*), 0.1 (*5*); (c) $\xi_h = 0.05$, $\xi_c = 0.01$, $V = 3.35$ K and $\varepsilon_0 = 4.01$ K (*1*), 3.25 K (*2*), 1.45 K (*3*).

4. Comparison with experiment

In this section we compare our theoretical results with well-known experimental measurements [3]. Our goal is to treat the specific heat of the purest ^{4}He crystal, so that we consider only two dependences corresponding to the lowest amount (1 ppb and 0.3 ppm) of ^{3}He impurities measured in Ref. 3. It can be seen from Fig. 1 of the mentioned paper that the both experimental dependences practically coincide each other (at least, visually).

First of all, we have to divide properly an anomalous contribution from the phonon part of heat capacity. This can be made through fitting the phonon heat Eq. (9) to the experimental curves of the paper [3]. We have made a copy of the discrete experimental points $C_V^{(\rm exp)}(T)$ just from the journal pictures of Ref. 3 using standard screen digitizer. It is possible to find exactly the pre-integral constant in Eq. (9). The volume of the experimental cell reported in [3] is 0.93 cm^3 at molar density of the sample equal to 20.46 cm^3/mol, so that the molar amount of ^{4}He in the cell is $\nu = 0.04545$ mol. As a result,

$$N_{2D} N_{1D} k_B = \nu R \,,$$

where $R = 8.31434\ \mathrm{J/(K{\cdot}mol)}$ is the universal gas constant. In this connection the only fitting parameters in the phonon part of the heat capacity is the frequency Ω in Eq. (9) (see also Eqs. (5)–(7)). The physical meaning of Ω is the effective elastic modulus of the polytypic medium. It should be noted that our model of Sec. 3.1 for phonon heat capacity is, in fact, an exact approach based on rigorous lattice dynamics [49]. The most advantage of this approach is that it does not include any uncertain parameters like Debye temperature θ_D. It is very important for crystalline helium where the estimated θ_D is much greater than the melting temperature of the solid.

The fitting of the phonon part has some specific peculiarities. As apply the formula Eq. (9) to the experiment, we have to take into account that the pure phononic behavior of the total heat capacity is expected above the local anomalous peak, i.e., the temperature $T_0 \approx 0.17$ K where the contribution of excessive heat becomes negligible small as compared to $C_{\rm ph}$ (the similar approach was used in [3]). Certainly, the value of T_0 can be a result of in some sense voluntary choice, and this temperature can be considered as an additional fitting parameter. We have made the fit between $C_{\rm ph}$ and experimentally determined heat capacity $C_V^{(\rm exp)}(T)$ within the temperature interval $T_0 \le T \le T_{\max} = 0.35$ K (where $T_{\max}$ is the upper temperature limit for the measurements reported in Ref. 3) through minimizing the average relative discrepancy

$$\delta_C = \frac{1}{T_{\max} - T_0} \int\limits_{T_0}^{T_{\max}} dT \frac{C_V^{(\rm exp)}(T) - C_{\rm ph}(T)}{C_{\rm ph}(T)}$$

in the chosen interval. It can be found that $\Omega = 9.66058$ K for the specimen with 1 ppb of ^{3}He impurity, and $\Omega = 9.72230$ K for 0.3 ppm of ^{3}He (in the both cases $\delta_C < 10^{-9}$). It is noticeable that the elastic modulus Ω is greater for crystal with greater amount of impurities (even for dilute ^{3}He–^{4}He solid solutions). It means that the doping of ^{3}He atoms leads to hardening in ^{4}He lattice. However, taken into account all the above-mentioned approximations and small difference between $C_{\rm ph}$ for the samples with 1 ppb and 0.3 ppm of ^{3}He, during the further considerations we put $\Omega =$ 9.7 K for both ^{3}He concentrations. The found Ω is in a good agreement with corresponding value for the temperature dependence of phonon pressure $P_{\rm ph}(T)$ derived in the papers Refs. 34, 35. Fig. 5 shows our phonon theory (solid line) fitted to the mentioned experimental data from Ref. 3 (blue pentagons for 0.3 ppm and red circles for 1 ppb, just as in the original paper [3]). In Fig. 6 all the data of Fig. 5 are re-plotted as a function of T^3-abscissa.

The anomalous excessive heat $C_{\rm ex}(T)$ as the difference between total heat capacity $C_V^{(\rm exp)}(T)$ (measured experimentally [3]) and pure phonon contribution $C_{\rm ph}(T)$ (calculated theoretically with Eq. (9)) is plotted on Figs. 5, 6 as the scattered sets of dark grey squares and grey hexagons,

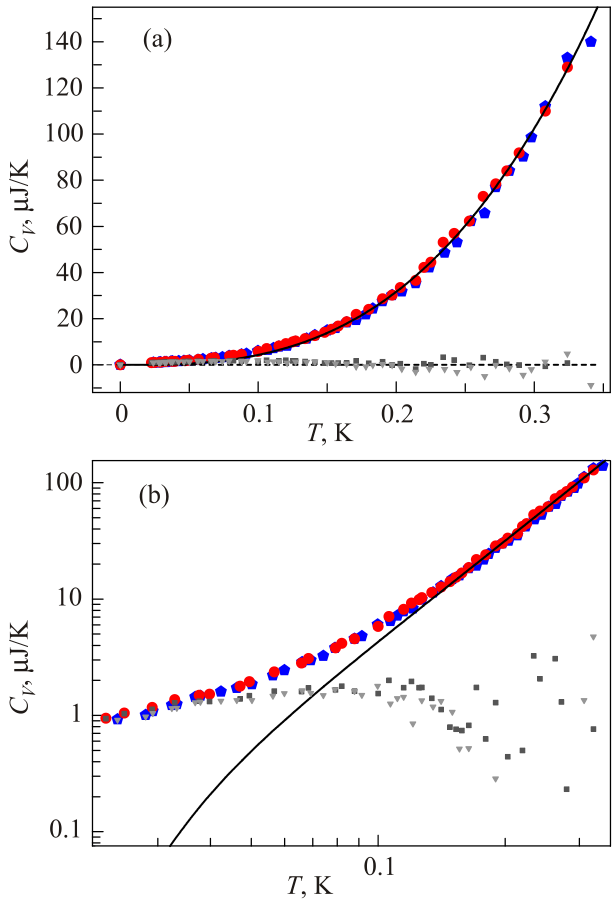

Fig. 5. (Color online) The phonon heat capacity $C_{\rm ph}(T)$ at $\Omega = 9.7$ K (solid line, theory) in comparison with total specific heat $C_V(T) = C_{\rm exp}(T)$ measured experimentally (scattered points: red circles belongs to 1 ppb sample and blue pentagons to 0.3 ppm one, correspondingly, just as it is in the paper [3]). Scattered boxes and triangles are excessive heat calculated theoretically as $C_{\rm ex} = C_{\rm exp} - C_{\rm ph}$ for 1 ppb sample (dark gray boxes) and 0.3 ppm (gray triangles). The dependences are plotted in linear (a) and double logarithmic (b) coordinates. Density fluctuations in impurity subsystem increase with temperature and ^{3}He concentration.

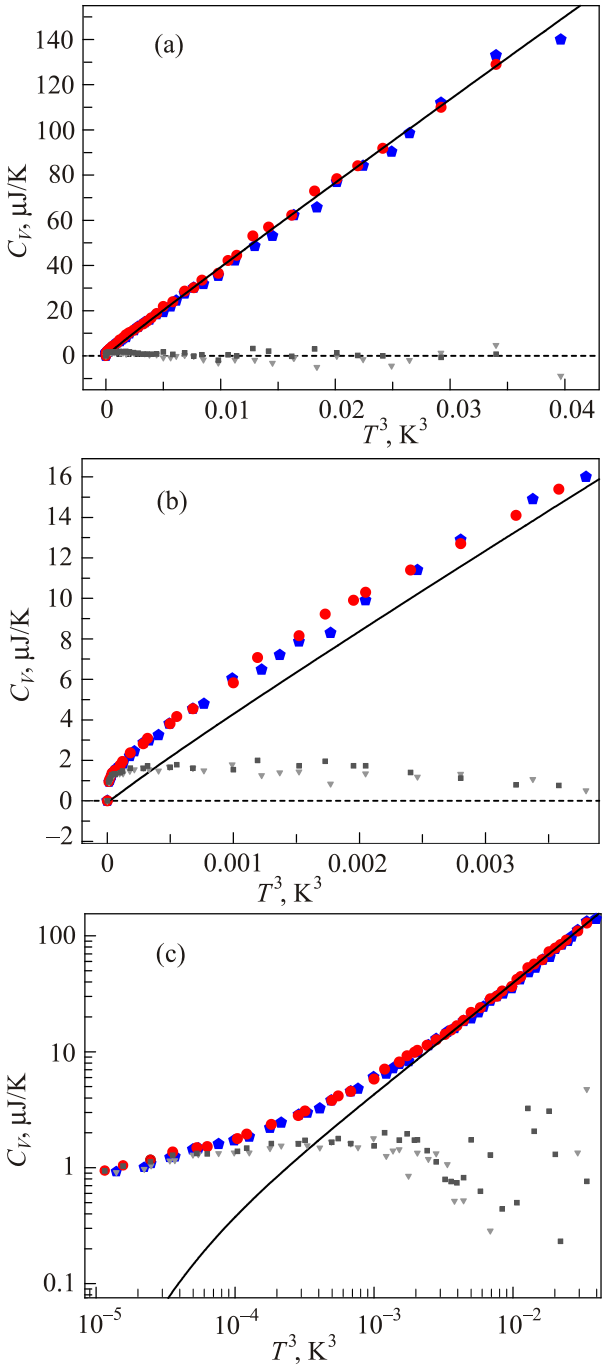

Fig. 6. (Color online) The re-plot of Fig. 5 versus T^3-abscissa: (a) reproduction of Fig. 5(a), (b) an initial part of the graph Fig. 6(a), (c) double logarithmic re-plot of Fig. 6(a). Solid line is $C_{\rm ph}(T)$ at $\Omega = 9.7$ K.

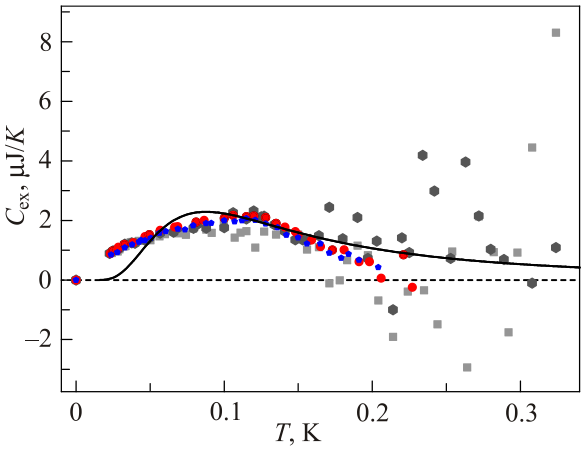

Fig. 7. (Color online) The peak of excessive heat capacity: theoretically calculated differences $C_{ex} = C_V^{(exp)} - C_{ph}$ for 1 ppb sample (gray boxes) and 0.3 ppm (dark hexagon) in combination with experimentally determined functions from the paper [3] (red circles for 1 ppb and blue pentagons for 0.3 ppm of ^{3}He, correspondingly). The solid line is theoretical fitting according to Eq. (17) at $\xi_h = 0.05$, $\xi_c = 0.01$, $\varepsilon_0 = 4.01$ K, $V = 3.33$ K, and $k_B N_{1D} = 4.51$ μJ/K.

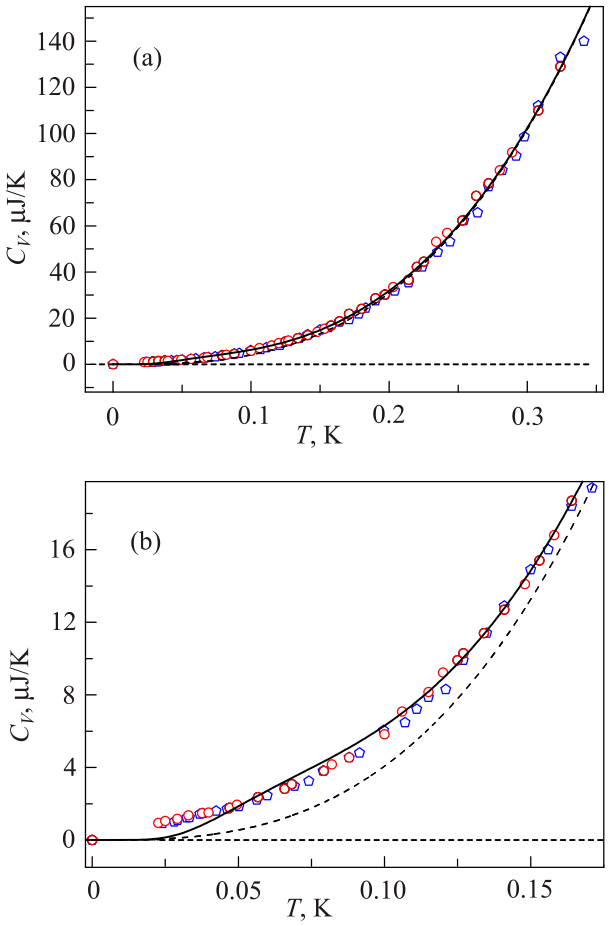

Fig. 8. (Color online) Theoretical fitting of the total heat capacity $C_V = C_{ph} + C_{ex}$ (solid line) within linear coordinates. The phonon part C_{ph} is represented by dashed line (parameters of this curve are similar to Figs. 5, 6). Fig. 8(b) shows the low-temperature part of the dependences.

belonging to the samples with 0.3 ppm and 1 ppb of ^{4}He, correspondingly. Figure 7 presents the obtained dependences $C_{ex}(T)$ in comparison with corresponding results of Ref. 3. When comparing the excessive heat from Fig. 2 of the paper Ref. 3 with the theory of Eq. (17) we have to take into account that these data [3] are specific heat normalized to one mole of helium, so that for our goals the given numbers should be re-calculated to the molar amount $\nu = 0.04545$ mol. Very important feature of experimentally measured $C_{ex}(T)$ is the exact coincidence between two dependences for 1 ppb and 0.3 ppm in the range of anomalous maximum (0.02–0.2 K) where the experimental curve is perfectly determined, whereas above 0.2 K the dispersion of the experimental points crucially increases, probably due to increase in fluctuations within impurity subsystem of the dilute solid solution (above 0.2 K the impurity subsystem of 1 ppb and 0.3 ppm solutions behaves like a homogeneous perfect gas).

Another uncertain factor is the number N_{1D} of 2D crystalline layers in the one-dimensional stack. As it follows from Fig. 4 the maximum height of the normalized excessive heat capacity does not depend practically on the values of all energetic parameters in Hamiltonian Eq. (10). So, the hight of this maximum can be fitted only by choosing the parameter N_{1D}. It has been found that the best fitting to the experiment is achieved at $k_B N_{1D} = 4.51$ μJ/K (see Fig. 7).

The dependence $C_{ex}(T)$ demonstrates a properly determined local maximum at low temperature, but at higher temperatures (above approximately 0.17 K) the scatter of experimental points becomes much higher and increases with temperature. This fact testifies that the density fluctuations in subsystem of ^{3}He impurities within even dilute ^{3}He–^{4}He solid solution rapidly increase with temperature, and the scattering is more essential in the mixed crystal with greater concentration of ^{3}He. It is a consequence of the great mobility of ^{3}He impuritons in ^{4}He matrix controlled by quantum diffusion, but in this connection we have to explain the properly systematic (in fact, fluctuationless) behavior of $C_{ex}(T)$ below 0.17 K (see Fig. 7).

Figure 8 demonstrates the total heat capacity $C_V(T) = C_{ph}(T) + C_{ex}(T)$ with theoretical fitting, and Fig. 9 gives the same pictures versus T^3-abscissa. The characteristic behavior of the excessive heat capacity will be discussed in the next section.

5. Discussion

The present work demonstrates that the apparent anomalies in thermodynamical and mechanical properties (which means a deviation from the normal phonon-caused behavior of a structurally perfect, defect-free crystal lattice) of solid hcp ^{4}He can be interpreted successfully within the well-

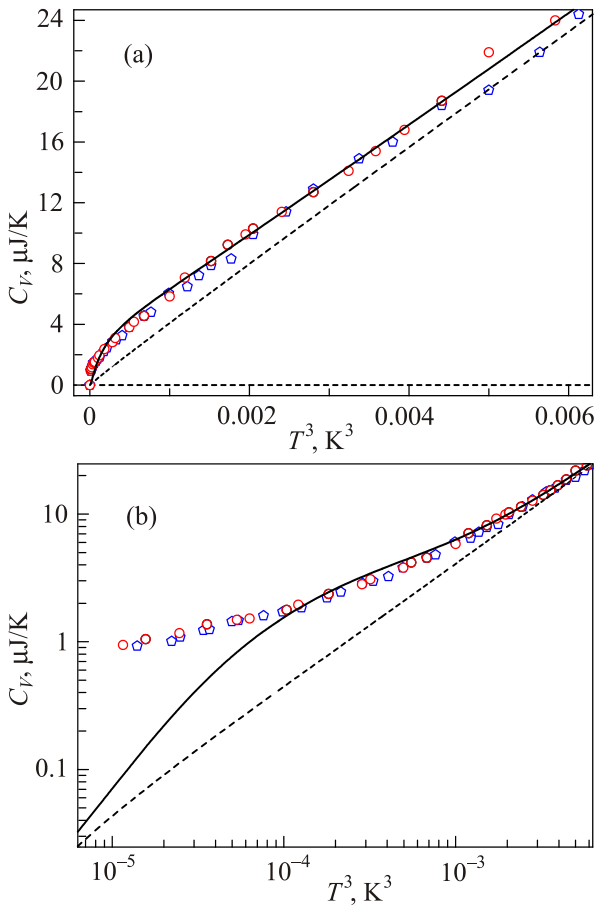

Fig. 9. (Color online) The re-plot of Fig. 8 (low-temperature part) versus T^3-abscissa.

known physical model of crystalline polytype built as a random stack of close-packed 2D layers on triangular lattice without breaking the principle of the closest packing in 3D geometry [37]. It is shown in [34] that hcp polytype can be treated as anisotropic elastic continuum with specific dispersion law in direction of disordered c axis. Previously, this model was applied [35] to interpret the discovered experimentally in Ref. 1 anomalous temperature dependences of pressure $P(T)$ in hcp ^{4}He crystal. In the present paper we explain the observed experimentally in Ref. 3 anomalies of heat capacity $C_V(T)$ of ^{4}He solid. It is noticeable that the anomalies of both solid ^{4}He thermodynamic functions, $P(T)$ and $C_V(T)$, were found in independent experiments [1,3], but at approximately similar temperatures (of order $\sim$0.1 K). It is noticeable that the various anomalies in mechanical (and acoustical) properties [27] of solid ^{3}He can be found just within the similar temperature interval 0.1–0.2 K. It means evidently that the all these phenomena have the common physical nature.

Thermodynamics and mechanics of crystalline solids are primarily structurally dependent properties, so that the reason of ultralow-temperature anomalies can be only some specific peculiarities of the hcp ^{4}He lattice (bcc ^{3}He crystals does not demonstrate the corresponding behavior). Crystallographic symmetry of the ideal lattice specifies the phonon spectrum based on the oscillatory degrees of freedom. Crystal lattice defects (vacancies, impurities, dislocations, stacking faults, etc.) produce their own degrees which replace or transform a part of phonon degrees from an initially perfect solid. All these phenomena are mostly pronounced in solid helium due to the isotopic purity and quantum nature of the ^{3}He–^{4}He compositions. The suggestion of additivity between phononic and excessive polytypic contributions to the total heat capacity of hcp ^{4}He should be considered as a variant of self-consistency for lattice dynamics which takes into account an effect of structural transformation in the multilayered polytype on the phonon spectrum of the system. As it is seen from Figs. 7–9, our model gives satisfactory semi-quantitative description for the temperature dependence of the excessive heat capacity $C_{ex}(T)$ with correct limits $C_{ex}(0) = 0$ and $C_{ex}(\infty) \to 0$. However, it is evident that the behavior of $C_{ex}(T)$ at $T \to 0$ is rather exponential like

$$C_{ex}(T) \sim T^{\alpha} \exp(-\tau/T), \quad |\alpha| \sim 1, \ \tau > 0, \qquad (18)$$

whereas the run of experimentally obtained curve is, probable, power-like (see Figs. 7, 9). It should be stressed that the power-like behavior is rather typical for the ultralow-temperature anomalies in thermodynamic functions of pure ^{4}He (but not for impurity subsystem), and this conclusion is supported by the results of corresponding fitting for the anomalous run of pressure at $T \to 0$ [1,35]. Nevertheless, the used here 1D quasi-Ising (lattice gas) model for multilayered polytype with interlayer interactions presents the reasonable physical interpretation for the excessive heat capacity caused by specific degrees of freedom due to packing transformation in hcp crystalline stack [34,35]. This model seems to be more pronounced as compared to predictions given by the set of the simple independent two-level systems [31,33]. More adequate alternative to the quasi-Ising approach for the polytype thermodynamics could be the model of self-consistent phonons (SCP) [55,56] which directly exploits the temperature evolution of lattice elastic constants during continuous structural transformation in the crystal which leads to a temperature-dependent phonon spectra and, hence, to the complicated thermodynamics of the helium solid.

Another question is the role of impurities in thermodynamics of the helium crystals. Due to the nature of the systems under study, the helium crystal mixture consists of only two isotopes, ^{3}He and ^{4}He (others molecular impurities would be inevitable either separated or frozen during preparation of the solid helium samples). The thermodynamics of the helium mixed crystals with an arbitrary isotopic composition was studied experimentally [57–59] and interpreted theoretically [60–62] as the density-fluctuations phenomena over a self-consistent regular solid solution [63–65] under isotopic phase separation. In this connection the most pro-

nounced achievement of the last decade is experimental studies [3,27] of the purest hcp ^{4}He crystals with low-temperature anomalous behavior which can not be associated directly with phase separation in dilute ^{3}He–^{4}He solid solution. Thus, to interpret the ultralow-temperature thermodynamic anomalies in the solid ^{4}He we have to point the physical degrees of freedom which are responsible for the corresponding phenomena.

It should be noted that the closed system built of N atoms possesses exactly $3N$ translational degrees of freedom, and in a real crystal all the degrees are re-distributed among all excitations (phonons, impuritons, dislocations, etc.) which can exist in the crystal. For example, to produce a Shottky's vacancy we have to "evaporate" one atom from the lattice, but in solid helium it is impossible because the helium specimen within the closed cell has fixed number of atoms (N = const). To produce a Frenkel's vacancy we have to translate an atom to an interstitial position, but the number of translational degrees in the whole system remains unchanged. Kinks and jogs on the edge of dislocation extra-plain are specific configurations built of atoms of the whole lattice with N = const. In this connection we can not interpret the excessive heat capacity as an "additional" effect from some "external" contribution. The thermodynamics of the excessive heat ("excessive" means the deviation from standard T^3-law) should be realized through re-distribution of existing degrees within a lattice with fixed number of atoms.

As it can be seen from Fig. 7, the lattice gas model (Eqs. (10), (17)) predicts an exponential run of $C_{\rm ex}(T)$ at $T \to 0$ [53,66,67], whereas the experimentally obtained dependence is rather power-like, so that the nature of excessive heat could be caused by some peculiarities of the helium phonon spectrum. According to a commonly used scheme of phonon thermodynamics the anomalous low-temperature contribution to the heat capacity can be obtained from increase in low-frequency density of states due to quasi-local excitations within the continuous phonon spectrum produced by a heavy impurity atoms [68–70]. The only question is of what the real object plays the role of the "heavy impurity" in our case of dilute ^{3}He–^{4}He mixed crystal. The square of specific frequency of a lattice atom (in Einstein approximation) is $\sim \kappa/M$, so that the quasi-local states are possible not only with increase in impurity mass M, but also with decrease of interatomic bonding κ [68]. In other words, we have to find certain low-energetic degrees of freedom to support the increase in phonon density of states within the low-frequency region and, as a result, a certain "softening" of the hcp ^{4}He lattice in the vicinity of 0.1–0.2 K.

The natural suggestion within the above-mentioned sense is to consider the impuriton contribution to the heat capacity of the system under study. As it is seen from estimations made in the Sec. 4, even small amount of ^{3}He impurity leads to observable stretching of the ^{4}He matrix. If ^{3}He concentration n_0 increases from 1 ppb to 0.3 ppm then the effective elastic constant Ω of the solid solution increases on 0.64% and changes slowly the smooth run of the total heat capacity, but this fact has not any visible influence on the anomalous low-temperature peak of $C_V(T)$. It seems that the position of the anomalous maximum $C_V(T)$ does not depend on the impurity concentration n_0, and this fact makes it possible to suggest that the additivity, $C_V = C_{\rm ph} + C_{\rm ex}$ (see Eq. (1)) is valid, at least, at $n_0 \ll 1$.

The non-monotonic behavior of $C_V(T)$ in the ^{3}He–^{4}He solid solutions is typical due to phase separation, and this phenomenon is studied in both experimental [57,59] and theoretical [61,62] aspects. The thermodynamic functions of the ^{3}He–^{4}He mixed crystals demonstrate an anomalous behavior due to increasing in fluctuations near the equilibrium phase separation temperature, and this effect of density fluctuations in the impurity subsystem can be detected not only in the heat capacity [57,61,62] but also in the temperature-dependent phonon pressure within the pre-separation region [71,72]. Moreover, as it follows from our previous results [53,61,62,71,72], the impurity contribution to the thermodynamic functions $C_V(T)$ and $P(T)$ of a ^{3}He–^{4}He mixed crystal can be considered as additive part (along with phonon contribution) to the corresponding functions within a whole temperature interval where the helium solid state exists. The phase separation temperature T_s of the solid solution can be estimated within self-consistent field (regular solution) approximation as [73]

$$T_s^{-1} = \frac{1-2n_0}{2T_c} \ln \frac{1-n_0}{n_0}, \qquad (19)$$

where n_0 is the ^{3}He concentration in the homogeneous (non-separated) solid solution, and T_c is critical temperature of the mixture (for ^{3}He–^{4}He solid solution the critical temperature measured experimentally [74,75] and estimated theoretically [60] is $T_c = 0.38$ K). At $n_0 = 10^{-9}$ (1 ppb) we have $T_s = 0.0367$ K, and at $n_0 = 0.3 \cdot 10^{-6}$ (0.3 ppm), respectively, $T_s = 0.0506$ K. Table 1 gives the values of T_s calculated according to Eq. (19) for all ^{3}He concentrations studied in Ref. 3. It can be seen that all values of the Table 1 are in good agreement with experimental data of Fig. 3 from Ref. 3, but increase in $C_V(T)$ due to phase separation at the lowest concentrations of ^{3}He appears over the low-temperature anomalous peak which does not change neither its position nor magnitude with variation of n_0 in wide range of concentrations. Nevertheless, this fact does not provide a way to conclude that the anomalous peak is absolutely independent on the presence of ^{3}He atoms in the ^{4}He matrix, because the impurities have a principal effect on the structural peculiarities and, hence, phonon spectrum of the hcp matrix, and give an effect to the phonon heat capacity within the whole temperature range (see Sec. 3.1). The hysteresis of the heat capacity found in Ref. 3 at $n_0 \geq 10$ ppm is evidently the consequence of a certain substructural trans-

Table 1. Separation temperatures T_s calculated with Eq. (19) for mixtures with concentrations n_0 studied in Ref. 3

n_0	1 ppb	0.3 ppm	10 ppm	30 ppm	100 ppm	500 ppm
T_s, K	0.0367	0.0506	0.066	0.073	0.0825	0.1

formations, just similar to the corresponding phenomena on $P(T)$ dependences of ^{3}He–^{4}He solid solutions with various concentrations [76,77].

The most pronounced evidence for the structurally dependent nature of the low-temperature thermodynamic anomalies in ^{4}He crystals is found in Ref. 3 (see Fig. 3 in this paper) hysteresis on $C_V(T)$ dependence during thermocycling of the samples with higher amounts of the ^{3}He impurities (10 ppm and 500 ppm). The 500 ppm hysteresis is wider than 10 ppm one, and this fact illustrate the concentration dependence of the phenomenon. It is clear that all hysteretic events are consequences of some temperature-dependent structural reconstructions of the lattice which contain the point dilatation centers [76,77]. Due to long-range elastic fields produced by dilatation center, the lattice dislocation stopped by the point impurity will be splitted in the matrix with small enough stacking-fault energy (SFE). The splitting means local transformation of the lattice with formation of Shockley's partial dislocations which restrict the stacking fault area the wider the lower is SFE. The stacking fault can be a center of condensation for vacancies or impurities in the crystal [26,78] (so-called Suzuki atmosphere), so that it can be a way to realize the mechanism of stress-induced phase separation in dilute ^{3}He–^{4}He solid solutions at very low temperature and very low concentrations of impurities. Heat capacity of these systems was interpreted theoretically in Ref. 53 using the model of impurity deposition on the dislocation lines. The stacking faults with partial dislocations accommodate the misfit on the boundary between secondary phase cluster and the host matrix, as a result the nucleus of the secondary phase is surrounded by a wide pile-up built of partial dislocations. In other words, we obtain a "*heavy*" lattice defect of mesoscopic dimensions whose configuration is temperature-dependent and whose evolution with temperature is a lattice transformation of martensitic type. Certainly, the corresponding structural transformations have a principal effect on the density of phonon states in the matrix and, finally, on the heat capacity of the crystal lattice even at very small amounts of the impurity component. Impurities, as the dilatation centers and clusters of the secondary phase behave like nuclei of structurally transformed lattice, and these lattice aggregations contribute into thermodynamics of the helium crystal. In this connection, it is interesting to note that the role of heavy impurity can be played by inclusions of an "intermediate phase" discovered experimentally in Ref. 79.

The similar situation takes place with vacancies which can be considered as impurities of zero mass in the host lattice. Coalescence of vacancies into vacancy discs which are so-called Frank loops [26] (Frank's partial dislocations [80]) is another channel to relax the internal stresses and external pressure in the crystal. The role of the vacancies in thermodynamics of helium crystals is a matter of discussions for a long time [20–24], but at present the problem remains still unsolved.

To interpret all above-mentioned processes we based on the hcp structure with easy glide along basal planes and high probability of structural transformation due to mutual shifts of the neighboring crystalline elements. This mechanism is closely related to deformation properties of ^{4}He known as "supersolid". The deformation of multilayered polytype is, in fact, similar to the flow mechanism of a simple liquid. Moreover, to make an elementary transformation act (for example, $...ABC\dot{A}BC... \rightarrow ...ABCBCA...$), there is no need to translate one half of a crystal (denoted by overdot) relative to another half of the whole solid, but it is enough to rotate an upper part of the crystal around c axis on $\pi/6$. Such a twist deformation is an analog of spiral dislocation source [26,37] which makes a structural transformation in the polytype due to mutual rotation between the neighboring 2D layers. It is a proper way for deformation of the crystal in restricted geometry, especially in a torsion oscillator. So, the easy glide of hcp ^{4}He is, in fact, superplasticity of the corresponding crystal caused by specifics of its crystalline structure. The pyramidal and prismatic dislocation glide (typical for perfect hcp lattice) is blocked due to disorder in packing of the 2D crystalline planes, and only splitting and broadening of stacking faults in basal planes is easily executed.

Ising model makes us possible to describe evolution of the heterophase structure of the polytype with temperature and gives correct limits as $C_{ex}(0) = 0$ and $C_{ex}(T \rightarrow \infty) \rightarrow 0$. However, as it is seen from Fig. 7, the calculated dependence $C_{ex}(T)$ at $T \rightarrow 0$ is rather exponential (see Eq. (18)) whereas experimental curve demonstrates rather power-like behavior. It is a consequence of the fact that the heat capacity of the crystal is resulted from existence of the propagating bulk lattice excitations (elastic waves, phonons). One-dimensional packing transformations in a stack of the close-packed planes form only structural "background" for three-dimensional lattice dynamics which has to be built with rigorous account of the oscillatory degrees of freedom in the planes of the stack. It is evidently complicated problem, and to the present time it remains, in fact, unsolved. Applications of the Ising model to the polytypic crystals [43,44] were mainly connected with structural transformations due to formation of 1D long-periodic

structures, but no description for thermodynamics of the system was proposed. In Ref. 31 the closely-related idea [33] of glassy-like phase (perfect gas of independent two-level systems) was applied to the heat capacity peak in ^{4}He. To describe the thermodynamics of solid helium, we present here the real physical model of multilayered crystalline hcp polytype which can be considered as a stack of bistable (or multistable) planes on triangular lattice and treated with exactly solved Ising model [52]. At the ideal ratio $c/a = \sqrt{8/3} = 1.63$ the difference in energy of *h*- and *c*-configurations exist only due to neighbors in third coordination sphere, so that principally in our description we probably have to use the Ising model with next nearest neighbors [43–46]. However, even in our simplest approach the lattice gas with interaction between nearest neighbors has an essential advantage as compared to the model of independent two-level systems with speculative density of states [31]. This advantage, evidently, is due to correct account of the packing entropy in the stack of the close-packed atomic layers with triangular lattice.

Anomalous behavior of phononic pressure $P_{\rm ph}(T)$ in solid ^{4}He experimentally obtained in Ref. 1 was interpreted within the model of hcp crystalline polytype in our paper Ref. 35.

6. Conclusions

Stacking faults and polytypic structures exist also in bcc lattice, but their structure is different as compared to hcp. bcc structures have their own peculiarities for relaxation of internal stresses, but sometimes solid ^{3}He demonstrates some special features in its thermodynamic and acoustic properties very similar to discussed above for ^{4}He. In addition, there are known a lot of phenomena which can be treated within polytypic approach for ^{3}He–^{4}He solid mixtures (both separated and homogeneous) of different concentrations. All this problems should be a matter of further research.

1. I.A. Degtyarev, A.A. Lisunov, V.A. Maidanov, V.Y. Rubanskii, S.P. Rubets, E.Ya. Rudavskiy, A.S. Rybalko, and V.A. Tikhii, *J. Exp. Theor. Phys*. **111,** 619 (2010).
2. A.A. Lisunov, V.A. Maidanov, V.Y. Rubanskii, S.P. Rubets, E.Ya. Rudavskiy, A.S. Rybalko, and E.S. Syrkin, *Fiz. Nizk. Temp*. **38**, 589 (2012) [*Low Temp. Phys*. **38**, 459 (2012)].
3. X. Lin, A.C. Clark, Z.G. Cheng, and M.H.W. Chan, *Phys. Rev. Lett*. **102**, 125302 (2009); Erratum: **103**, 259903 (2009).
4. X. Lin, A.C. Clark, and M.H.W. Chan, *Nature* (*London*) **449**, 1025 (2007).
5. A.C. Clark and M.H.W. Chan, *J. Low Temp. Phys*. **138**, 853 (2005).
6. A.V. Balatsky, M.J. Graf, Z. Nussinov, and S.A. Trugman, *Phys. Rev. B* **75**, 094201 (2007).
7. D.O. Edwards and R.C. Pandorf, *Phys. Rev*. **140**, A816 (1965).
8. J. Beamish, *J. Low Temp. Phys*. **168**, 194 (2012).
9. X. Rojas, C. Pantalei, H.J. Maris, and S. Balibar, *J. Low Temp. Phys*. **158**, 478 (2010).
10. P.-C. Ho, I.P. Bindloss, and J.M. Goodkind, *J. Low Temp. Phys*. **109**, 409 (1997).
11. Z. Nussinov, A.V. Balatsky, M.J. Graf, and S.A. Trugman, *Phys. Rev. B* **76**, 014530 (2007).
12. A.C. Clark, J.T. West, and M.H.W. Chan, *Phys. Rev. Lett*. **99**, 135302 (2007).
13. J. Day, O. Syshchenko, and J. Beamish, *Phys. Rev. B* **79**, 214524 (2009).
14. F. Tsuruoka and Y. Hiki, *Phys. Rev. B* **20**, 2702 (1979).
15. J.R. Beamish and J.P. Franck, *Phys. Rev. B* **26**, 6104 (1982).
16. J.R. Beamish and J.P. Franck, *Phys. Rev. B* **28**, 1419 (1983).
17. S. Balibar, A.D. Fefferman, A. Haziot, and X. Rojas, *J. Low Temp. Phys*. **168**, 221 (2012).
18. V.N. Grigor'ev, V.A. Maidanov, V.Y. Rubanskii, S.P. Rubets, E.Ya. Rudavskiy, A.S. Rybalko, and V.A. Tikhii, *Fiz. Nizk. Temp*. **34**, 431 (2008) [*Low Temp. Phys*. **34**, 344 (2008)].
19. I. Iwasa, H. Suzuki, T. Nakajima, S. Suzuki, M. Ando, I. Yonenaga, M. Takebe, and K. Sumino, *J. Phys. Soc. Jpn*. **56**, 4225 (1987).
20. R.O. Simmons, *J. Phys. Chem. Solids* **55**, 895 (1994).
21. E.Y. Rudavskii, V.N. Grigor'ev, A.A. Lisunov, V.A. Maidanov, V.Y. Rubanskii, S.P. Rubets, A.S. Rybalko, and V.A. Tikhii, *J. Low Temp. Phys*. **158**, 578 (2010).
22. V.N. Grigor'ev, V.A. Maidanov, V.Yu. Rubanskii, S.P. Rubets, E.Ya. Rudavskii, A.S. Rybalko, Ye.V. Syrnikov, and V.A. Tikhii, *Phys. Rev. B* **76**, 224524 (2007).
23. Ye.O. Vekhov, V.N. Grigor'ev, V.A. Maidanov, N.P. Mikhin, V.Yu. Rubanskii, S.P. Rubets, E.Ya. Rudavskii, A.S. Rybalko, Ye.V. Syrnikov, and V.A. Tikhii, *Fiz. Nizk. Temp*. **33**, 835 (2007) [*Low Temp. Phys.* **33**, 635 (2007)].
24. V.N. Grigor'ev and Ye.O. Vekhov, *J. Low Temp. Phys*. **149**, 41 (2007).
25. J. Friedel, *Dislocations*, Pergamon, NY (1964).
26. J.P. Hirth and J. Lothe, *Theory of Dislocations*, McGraw-Hill, New York (1970).
27. F. Souris, A.D. Fefferman, A. Haziot, N. Garroum, J.R. Beamish, and S. Balibar, *J. Low Temp. Phys*. **178**, 149 (2015).
28. V. Zhuchkov, A.A. Lisunov, V.A. Maidanov, A.S. Neoneta, V.Y. Rubanskii, S.P. Rubets, E.Ya. Rudavskiy, and S.N. Smirnov, *Fiz. Nizk. Temp*. **41**, 223 (2015) [*Low Temp. Phys*. **41**, 169 (2015)].
29. A. Lisunov, V. Maidanov, V. Rubanskyi, S. Rubets, E. Rudavskii, S. Smirnov, and V. Zhuchkov, P*hys. Rev. B* **92**, 140505(R) (2015).
30. A.A. Lisunov, V.A. Maidanov, V.Yu. Rubanskyi, S.P. Rubets, E.Ya. Rudavskiy, and S.N. Smirnov, *Fiz. Nizk. Temp*. **42**, 1372 (2016) [*Low Temp. Phys.* **42**, 1075 (2016)].
31. J.-J. Su, M.J. Graf, and A.V. Balatsky, *J. Low Temp. Phys*. **159**, 431 (2010).
32. A.V. Balatsky, M.J. Graf, Z. Nussinov, and J.-J. Su, *J. Low Temp. Phys*. **172**, 431 (2013).
33. A.F. Andreev, *JETP Lett*. **159**, 431 (2007).
34. T.N. Antsygina, M.I. Poltavskaya, and K.A. Chishko, *Fiz. Nizk. Temp*. **41**, 743 (2015) [*Low Temp. Phys*. **41**, 575 (2015)].

35. K.A. Chishko, T.N. Antsygina, and M.I. Poltavskaya, *J. Low Temp. Phys*. **187**, 468 (2017).
36. N.V. Belov, *The Structure of Ionic Crystals and Metallic Phases*, USSR Academy of Sciences (1947) (In Russian).
37. A.R. Verma and P. Krishna, *Polymorphism and Polytypism in Crystals*, Willey, NY (1966).
38. B.I. Nikolin, *Multilayered Structures and Polytypism in Metallic Alloys*, Naukova Dumka, Kiev (1984) (in Russian).
39. V.A. Mikheev and V.A. Slyusarev, *Fiz. Nizk. Temp*. **7**, 379 (1981) [*Sov. J. Low Temp. Phys*. **7**, 186 (1981)].
40. V.A. Mikheev, V.A. Maidanov, and N.P. Mikhin, *Fiz. Nizk. Temp*. **7**, 670 (1981) [*Sov. J. Low Temp. Phys*. **7**, 330 (1981)].
41. N.P. Mikhin and V.A. Maidanov, *J. Low Temp. Phys.* **148**, 701 (2007).
42. Ya.D. Vishnyakov, *Crystal Structure of Stacking Faults*, Metallurgia, Moscow (1970) (in Russian).
43. G.D. Price and J. Yeomans, *Acta Crystallogr*. **B40**, 448 (1984).
44. J.M. Yeomans and G.D. Price, *Bull. Mineral*. **109**, 3 (1986).
45. W. Selke, *Z. Phys. B: Condens. Matter* **57**, 49 (1984).
46. D. DeFontaine and J. Kulik, *Acta Metallurgica* **33**, 145 (1985).
47. L.D. Landau and E.M. Lifshitz, *Statistical Physics*, Pergamon Press, Oxford (1958).
48. J.A. Reissland, *Physics of Phonons*, John Willey, London (1973).
49. H. Böttger, *Princips of the Theory of Lattice Dynamics*, Academie-Verlag, Berlin (1983).
50. T.N. Antsygina, I.I. Poltavskiy, M.I. Poltavskaya, and K.A. Chishko, *Fiz. Nizk. Temp*. **28**, 621 (2002) [*Low Temp. Phys.* **28**, 442 (2002].
51. L. Brillouin and M. Parodi, *Propagation des ondes dans les milieux périodiques*, Paris (1956).
52. R.J. Baxter, *Exactly Solved Models in Statisical Mechanics*, Academic Press, London (1982).
53. T.N. Antsygina, V.A. Slusarev, and K.A. Chishko, *Fiz. Nizk. Temp*. **21**, 583 (1995) [*Low Temp. Phys.* **21**, 453 (1995)].
54. B.N. Parlett, *The Symmetric Eigenvalue Problem*, Prentice-Hall, Inc., NJ (1980).
55. N.R. Werthamer, *Self-Consistent Phonon Theory of Rare Gas Solids*, in: Rare Gas Solids, V.1, p. 265, M.L. Klein and J.A. Venables (eds.), London (1976).
56. R. Guyer, *Solid State Phys*. **23**, 413 (1969).
57. D.O. Edwards, A.S. McWilliams, and J.G. Daunt, *Phys. Rev. Lett*. **9**, 195 (1962).
58. D.O. Edwards and M.S. Pettersen, *J. Low Temp. Phys*. **87**, 473 (1992).
59. R. Schrenk, O. Friz, Y. Fudjii, E. Siskakis, and F. Pobell, *J. Low Temp. Phys.* **84**, 133 (1991).
60. T.N. Antsygina, K.A. Chishko, and V.A. Slusarev, *JETP* **92**, 93 (2001).
61. T.N. Antsygina, V.A. Slusarev, and K.A. Chishko, *Phys. Solid State* **40**, 325 (1998).
62. T.N. Antsygina, K.A. Chishko, and V.A. Slusarev, *J. Low Temp. Phys.* **111**, 577 (1998).
63. I. Prigogine, *The Molecular Theory of Solutions*, North-Holland, Amsterdam (1957).
64. E.A. Guggenheim, *Mixtures*, Clarendon Press, Oxford (1952).
65. W.J. Mullin, *Phys. Rev. Lett*. **20**, 254 (1968).
66. T. Hill, *Statistical Mechanics*, McGraw-Hill, NY (1956).
67. R. Kubo, *Statistical Mechanics*, North Holland, Amsterdam (1965).
68. I.M. Lifshitz and A.M. Kosevich, *Rep. Progr. Phys*. **29**, 217 (1966).
69. I.A. Gospodarev, V.I. Grishayev, A.V. Eremenko, M.S. Klochko, A.V. Kotlyar, E.V. Manzheliy, E.S. Syrkin, and S.B. Fedosyev, *Fiz. Nizk. Temp*. **40**, 1296 (2014) [*Low Temp. Phys*. **40**, 1013 (2014)].
70. I.A. Gospodarev, V.I. Grishayev, A.V. Kotlyar, K.V. Kravchenko, E.V. Manzheliy, E.S. Syrkin, and S.B. Feodosyev, *Fiz. Nizk. Temp*. **34**, 829 (2008) [*Low Temp. Phys*. **34**, 655 (2008)].
71. T.N. Antsygina, A.A. Lisunov, V.A. Maidanov, V.Y. Rubanskyi, S.P. Rubets, E.Ya. Rudavskii, and K.A. Chishko, *Physica B: Condens. Matter* **406**, 3870 (2011).
72. T.N. Antsygina, V.N. Grigoriev, V.A. Maidanov, A.A. Pensev, S.P. Rubets, E.Ya. Rudavskii, A.S. Rybalko, Ye.V. Syrnikov, and K.A. Chishko, *Fiz. Nizk. Temp*. **31**, 1395 (2005) [*Low Temp. Phys*. **31**, 1059 (2005)].
73. I. Prigogine and R. Defay, *Chemical Thermodynamics*, Longman, London (1973).
74. P.M. Tedrow and D.M. Lee, *Phys. Rev.* **181**, 399 (1969).
75. D.O. Edwards and S. Balibar, *Phys. Rev. B* **39**, 4083 (1989).
76. A.P. Birchenko, Ye.O. Vekhov, N.P. Mikhin, and K.A. Chishko, *Fiz. Nizk. Temp*. **35**, 1177 (2009) [*Low Temp. Phys*. **35**, 914 (2009)].
77. J.H. Vignos and H.A. Fairbank, *Phys. Rev*. **147**, 185 (1966).
78. H. Suzuki, *Sci. Repts. Tohoku Univ*. **A4**, 455 (1952).
79. N.P. Mikhin, A.P. Birchenko, A.S. Neoneta, E.Y. Rudavskii, and V.G. Baidakov, *J. Low Temp. Phys.* **175**, 154 (2014).
80. F.C. Frank and J.F. Nicholas, *Philos. Mag*. **44**, 1213 (1953).